Dynamic simulation of an original Joule cycle liquid pistons hot air Ericsson engine

Max Ndamé Ngangué, P Stouffs

Version of Record: https://www.sciencedirect.com/science/article/pii/S0360544219319887
Manuscript_c4c88f50f4d35a2af469ac62f4439ec4

DYNAMIC SIMULATION OF AN ORIGINAL JOULE CYCLE LIQUID PISTONS HOT AIR ERICSSON ENGINE

Max Ndamé Ngangué, *Pascal Stouffs

Univ. Pau & Pays Adour/E2S UPPA, Laboratoire de Thermique, Energétique et Procédés-IPRA, EA1932, F-64000 Pau, France

* Corresponding author: pascal.stouffs@univ-pau.fr
Phone: +33 559407124 Mobile phone: +33 625876307

Abstract:

An Ericsson engine is an external heat supply engine working according to a Joule thermodynamic cycle. It is based on reciprocating piston-cylinder machines. Such engines are especially interesting for low power solar energy conversion, micro-CHP from conventional fossil fuels or from biomass and waste heat recovery. An innovative configuration has been designed where the mechanical pistons are replaced by liquid pistons. The engine is composed of two U-shape tubes partially filled with water, one for the compression spaces and one another for the expansion spaces. A thermodynamic model of the engine is developed. The model takes into account the dynamics of the liquid columns. It is shown that the engine indicated efficiency decreases when the rotation speed increases. The sign of the instantaneous torque on the flywheel changes four times per cycle, calling for a heavy flywheel. When the rotation speed increases above the natural frequency of oscillation of the liquid columns, the influence of the liquid pistons inertia is growing. Its impact is globally opposite to the one of the pressure in the cylinders. So, the effect of the inertia of the liquid columns is to reduce the amplitude of the torque variations.

Keywords:

Hot air engines, Joule cycle engines, Ericsson engines, liquid pistons.

1. Introduction

The world is going through an energy crisis due to a massive population growth, the economic rise of emerging countries, the depletion of fossil fuel reserves, and the proliferation of conflicts in parts of the world because of the interest of some powerful countries in fossil fuels. Yet according to the International Energy Agency (IEA) in its 2014 report [1], fossil fuels account for just over 81% of the energy consumed in the world. Their exploitation is largely responsible for the current environmental situation marked by high pollution and abnormal global warming. It becomes crucial to develop “clean” power generation technology.

Therefore, a lot of research is devoted to find alternative energy sources to fossil fuels. In this context, micro- or mini-cogeneration from renewable energy sources is an important investigation field to deal with this problem.

The purpose of this paper is to assess the performance of an original configuration of an Ericsson engine equipped with liquid pistons. This kind of engine is thought to be suited for small scale conversion of biomass or solar energy into electricity (up to …10 kW).

1.1. The Ericsson engine

The family of hot air engines is divided in two subgroups: the Stirling engines, invented in 1816, have no valves whereas Ericsson engines, invented in 1833 have valves in order to isolate the cylinders [2]. The Ericsson engine is defined as an external heat supply reciprocating engine equipped with valves. It is generally composed of a compression cylinder with automatic or actuated valves, a heat recovery exchanger, a hot source heat exchanger, and an expansion cylinder equipped with actuated valves. According to the technological design considered, the Ericsson engine can have different configurations. Figure 1 (a) presents the general configuration, whereas figure 1 (b) presents an open cycle design. In some cases, the Ericsson engine is built without any recuperator heat exchanger.

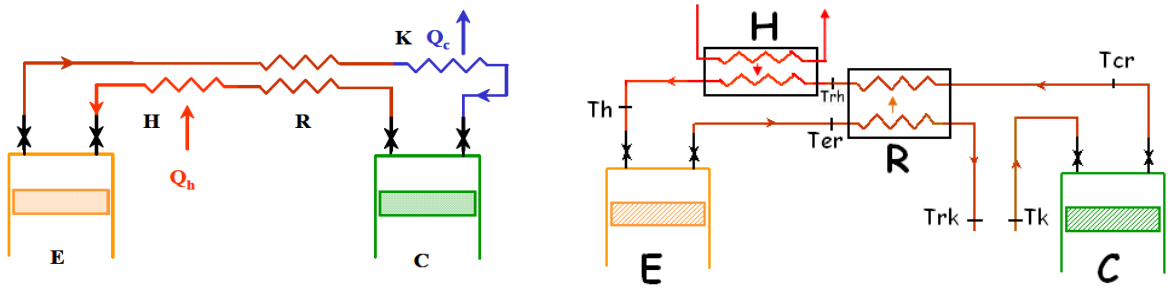

(a) (b)

Fig. 1. General Ericsson engine configuration (a) and open cycle Ericsson engine configuration (b).

The elements of the Ericsson engines are the followings [3]:

- E: Expansion cylinder, equipped with actuated valves;
- H: Heater, heat exchanger between the hot source and the working fluid;
- R: Recuperator, heat recovery exchanger;
- K: Cooler, heat exchanger between the working fluid and the cold source;
- C: Compression cylinder equipped with automatic or actuated valves.

The valves give some advantages to the Ericsson engine. Amongst them, the most important one is that the heat exchangers are not to be considered as unswept dead volumes whereas the Stirling engine designer is faced to the difficult compromise between heat exchanger transfer area maximization and heat exchanger volume minimization [3].

There is a renewed interest in Ericsson engine since different studies have shown that this engine could have high energy performances, similar of those of Stirling engines, in the low power range, but with lower internal pressure levels [4]. On the other hand, the Ericsson engine is suitable for the production of small scale energy using renewable energy resources such as biomass [4-6], or solar energy [6-10].

1.2. Liquid pistons

Since the pioneer work of C. D. West, liquid pistons have been widely studied in the case of Fluidyne Stirling engines for pumping applications [11-25], hybrid solid-liquid pistons Stirling [26-29] or steam [30] engines, liquid pistons compressors [31-34], two-phase thermo-fluidic engines [35-45] heat pumps or cooling devices [45-46], and desalination plants [47].

1.3. The proposed liquid pistons configuration

An innovative configuration of a hybrid solid-liquid pistons Ericsson engine is proposed (Fig. 2). Compared to Fluidyne Stirling engines, the Ericsson liquid pistons configuration with valves allows to achieve higher pressure amplitudes in the engine, since the heat exchangers are not dead unswept volumes [3]. This hot air liquid pistons Ericsson engine is composed of two compression cylinders (C) consisting of a U-shape tube partially filled with liquid and closed by a cylinder head in the upper part, two expansion cylinders (E) similarly made of a U-shape tube, a counter flow heat recovery exchanger (R), a heater (H), a hot gas buffer tank (R.A) and a flywheel (V).

The liquid columns being in phase opposition, the descent of the piston in one of the enclosures corresponds to the rise of the piston in the other, and vice versa. Each U-tube contains two working

spaces, for compression (C) or expansion (E), of the working fluid. So the system is composed of two elementary Ericsson engines working in phase opposition. The air enters the compression chambers at the temperature T_k and at atmospheric pressure, and comes out compressed at the temperature T_{cr} to be preheated in the counter-current heat recovery heat exchanger R up to the state T_{rh} . It then passes into the heater H where it is heated by means of an external heat source. The tank RA provides buffer storage of air during the process. The hot air enters the expansion cylinder E at temperature T_h and comes out at temperature T_{er}.

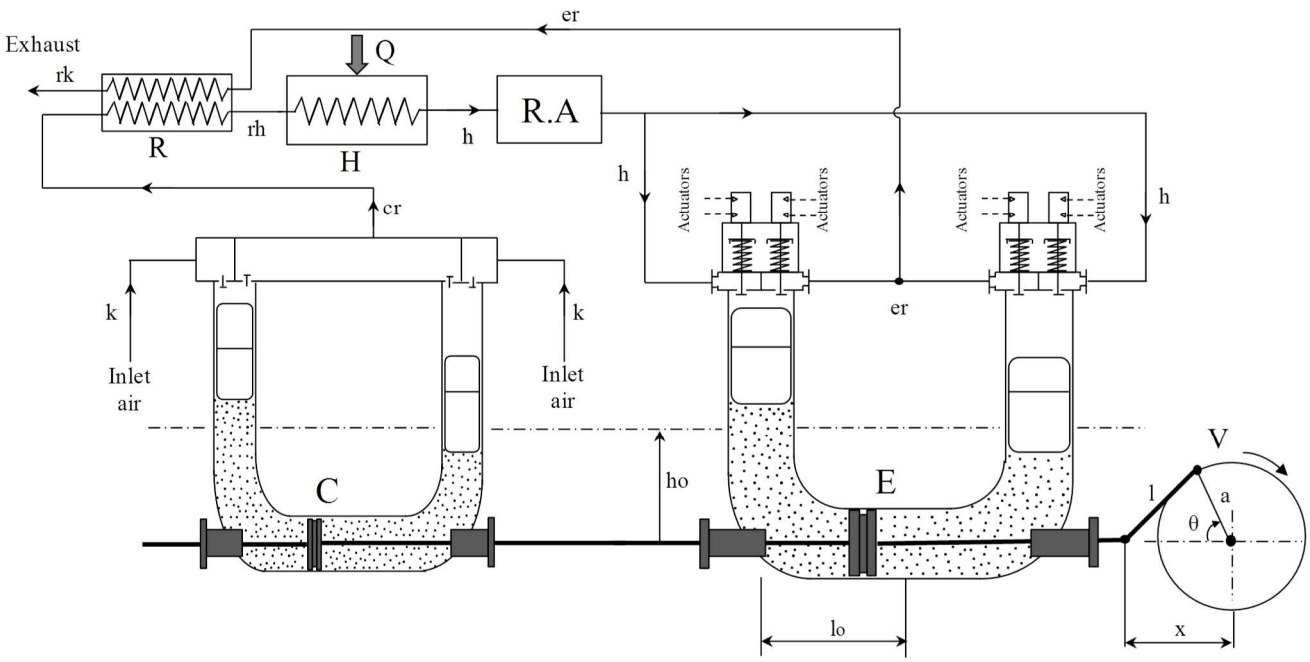

Fig. 2. Configuration of the proposed liquid pistons Ericsson engine.

The compression working spaces can be equipped with automatic or actuated valves. The expansion cylinders can be equipped with actuated valves or with a very simple distribution system, known as 'bash valve' [9]. In the present study, actuated valves are considered for the expansion cylinders.

It is assumed that this kind of engine is easier to build than conventional mechanical engine. One of the main advantage of the liquid pistons is the perfect tightness between the working fluid and the cylinder around the moving piston. The small liquid leak in the annular gap around the solid piston at the bottom of the U-tube has a much smaller influence on the performance of the engine than leaks of the working fluid around a conventional piston. So there is no need of several rings on the solid piston. Therefore it has been shown that such engine could have a very good mechanical efficiency [32].

The main characteristics of the modelled engine are presented in Table 1. These data correspond to the ones of a prototype under construction. They are based on the know-how gained by previous experimental and theoretical studies in the laboratory [9-10, 48]. The compression swept volume is $V_{C,comp} = 4\ 10^{-3}$ m^3 in each part of the U-tube (left and right) while the expansion swept volume is $V_{C,exp} = 6\ 10^{-3}$ m^3 in each part of the U-tube.

In order to have the same natural frequency of the liquid pistons in both the compression and expansion U-tubes, identical equilibrium liquid column height h_0 and horizontal U-tube length l_0 are considered. The geometrical data presented in Table 1 lead to a natural frequency of the oscillation of the liquid columns of $f_0 = 0.63$ Hz, which corresponds to a rotational speed of 37.8 rpm. The expected shaft power for this rotational speed is about 150 W.

The system is designed as to have a nominal pressure p_H in the heater of about 300 kPa, as this has been considered as a good compromise between engine size and engine performance [6]. It is well known that for low compression ratios, the Joule cycle efficiency can be increased by adding a

recovery exchanger in order to preheat the compressed air before entering the heater. A recovery heat exchanger with an effectiveness $\varepsilon_R = 0.85$ is considered. It is assumed that this effectiveness is a good compromise between the investment cost and the benefit on cycle efficiency.

Table 1. Main characteristics of the engine

Geometrical data		Operation data	
Crank radius, a	0.125 m	Working fluid	air
Connecting rod length, l	0.5 m	Liquid	water
Compression tube diameter, D_{comp}	0.143 m	Heat recovery effectiveness, ε_R	0.85
Expansion tube diameter, D_{exp}	0.175 m	Comp. inlet temperature, T_k	300 K
Compress. swept volume (1 cylinder)	4 dm^3	Heater inlet temperature, T_h	633.15 K
Expansion swept volume (1 cylinder)	6 dm^3	Comp. inlet pressure, p_k	100 kPa
Comp. relative dead volume, $\zeta_{d,comp}$	0.4	Expander outlet pressure, p_{rk}	100 kPa
Exp. relative dead volume, $\zeta_{d,exp}$	0.4		
Volumetric compress./expansion ratio	3.5		
Comp. equilib. liquid height, $h_{0,comp}$	0.225 m		
Comp. horizontal tube length, $l_{0,comp}$	0.4 m		
Exp. equilib. liquid height, $h_{0,exp}$	0.225 m		
Exp. horizontal tube length, $l_{0,exp}$	0.4 m		

2. The model

2.1. Thermodynamics analysis

Different approaches can be used to model Ericsson engines. Global analyses (see for instance [4, 9, 10, 48]) use simple assumptions for the thermodynamic processes in each of the components of the engine. These models give relationships between the geometrical characteristics of an Ericsson engine (cylinder capacities, dead volumes), its operating parameters (maximum pressure and temperature) and its energy performance (power, efficiency) which are useful in order to design an engine. Some other analyses are based on analogies between the linearised, spatially lumped governing equations for thermal and fluid transport, and descriptions of linear, passive electrical components [38-42]. All these models give cycle-averaged values of the variables describing the systems. Some models consider the dependence of the variables on the crankshaft angle [49-52]. These 'intra-cycle' models are sometimes somewhat improperly referred to as 'dynamic models'. One study deals with the intra-cycle modelling of a liquid piston Stirling engine [53], but no study is devoted to the intra-cycle modelling of a liquid pistons Ericsson engine. The originality of the present analysis is to couple a classical intra-cycle model of an Ericsson engine with the equations of the dynamics of the liquid pistons.

2.1.1. General assumptions

It is assumed that a float is positioned on each liquid column. These floats have a length at least equal to the stroke of the engine $2a$, in order to separate the upper hot part of the tube, containing the working fluid, and the lower cold part of the tube containing the liquid. So any heat or mass transfer between the working fluid and the liquid piston can be neglected. The working fluid is air assuming to obey the ideal gas law. The heat capacity of air is assumed to be dependent on the temperature. The viscous losses are neglected in the working fluid (air) but not in the liquid pistons (water). The compression and expansion of air in the cylinder are considered as adiabatic and reversible processes. The pressure in the heat exchangers is assumed to be constant.

2.1.2. Kinematic mechanism

A usual mechanism with a crankshaft of radius a and a connecting rod of length l is considered. However, for the sake of simplicity, it is assumed that the length of the connecting rod is much larger than the crankshaft radius $l >> a$. So the cycles in the left hand side of the expansion and compression tubes can be considered as identical to the ones on the right hand side of the tubes, with a phase shift of 180°. According to Figure 2, the position x of the piston as a function of the crank angle is given by (1):

$$x = a\left(\cos(\theta) + \sqrt{\lambda^2 - \sin^2(\theta)}\right), \qquad (1)$$

In this equation, θ is the instantaneous crank angle and λ is the ratio of the connecting rod length to the crank radius $\lambda = l/a$. The crank angle $\theta = 0$ corresponds to the top dead centre (TDC) of the left part of the compression and expansion tubes (Fig. 2). We assume that the crankshaft is equipped with a large enough flywheel so that the angular speed ω can be considered as constant in (2):

$$\theta = \omega t, \qquad (2)$$

The piston speed (3) and the piston acceleration (4) can be derived from Eq. (1):

$$\frac{\mathrm{d}x}{\mathrm{d}t} = \omega\frac{\mathrm{d}x}{\mathrm{d}\theta} = -a\,\omega\sin(\theta)\left(1 + \frac{\cos(\theta)}{\sqrt{\lambda^2 - \sin^2(\theta)}}\right), \qquad (3)$$

$$\frac{\mathrm{d}^2x}{\mathrm{d}t^2} = \omega^2\frac{\mathrm{d}^2x}{\mathrm{d}\theta^2} = -a\,\omega^2\left(\cos(\theta) + \frac{\cos^2(\theta) - \sin^2(\theta)}{\sqrt{\lambda^2 - \sin^2(\theta)}} + \frac{\sin^2(\theta)\cos^2(\theta)}{\left(\sqrt{\lambda^2 - \sin^2(\theta)}\right)^3}\right), \qquad (4)$$

From the knowledge of the piston position, the instantaneous volume of each cylinder can be easily derived. For instance, the instantaneous volume of the left and right compression cylinders are given by (5) and (6):

$$V_{comp,left} = \frac{\pi D_{comp}^2}{4}\left(2\,a\,\zeta_{d,comp} + l + a - x\right), \qquad (5)$$

$$V_{comp,right} = \frac{\pi D_{comp}^2}{4}\left(2\,a\,\zeta_{d,comp} - l + a + x\right), \qquad (6)$$

where $\zeta_{d,comp}$ is the relative dead (unswept) volume of the compressor. The relative dead volume is defined as the dead volume divided by the piston course and by the tube section. The diameter of the tube is constant in the compression and expansion cylinders and the dead volumes are identical in both compression –respectively expansion cylinders.

2.1.3. Working spaces in the tubes

The admission and exhaust valve lift is assumed to follow half a sinusoid. The maximum lifts, the valve diameters and the opening and closing angles are imposed as data for each cylinders. The air mass flow rate through a valve is given by (7):

$$\dot{m} = A\,C_d\,p\left(\frac{2\gamma}{(\gamma-1)\,rT}\left(R^{\frac{2}{\gamma}} - R^{\frac{\gamma+1}{\gamma}}\right)\right)^{\frac{1}{2}}, \qquad (7)$$

where A is the instantaneous flow area through the valve, C_d is a flow coefficient, γ is the ratio of constant pressure to constant volume specific heat, r is the ideal gas constant per unit mass, p and T are the upstream fluid pressure and temperature and R is the pressure ratio. The pressure ratio R is limited by the critical pressure ratio (8):

$$R_{crit} = \left(\frac{2\gamma}{\gamma+1} \right)^{\frac{\gamma-1}{\gamma}}, \qquad (8)$$

The fluid state in the working spaces is described by means of the mass balance equation (9), the energy equation (10) and the equation of state for an ideal gas (11).

$$\frac{\mathrm{d}m}{\mathrm{d}t} = \dot{m}_{adm} - \dot{m}_{exh}, \qquad (9)$$

where m is the instantaneous mass of fluid in the cylinder, $\dot{m}_{adm}$ the mass flow rate through the admission valve and $\dot{m}_{exh}$ the mass flow rate through the exhaust valve.

$$m \frac{\mathrm{d}u}{\mathrm{d}t} + u \frac{\mathrm{d}m}{\mathrm{d}t} = \dot{m}_{adm}\, h_{adm} - \dot{m}_{exh}\, h_{exh} - p \frac{\mathrm{d}V}{\mathrm{d}t}, \qquad (10)$$

where u and h are the internal energy and the enthalpy per unit mass. In the energy equation (10), the kinetic and potential energies are neglected and there is no heat transfer term as the processes in the cylinders are assumed to be adiabatic.

$$p = \rho\, r\, T, \qquad (11)$$

where ρ is the fluid density.

2.1.4. The whole engine

In order to simulate one elementary engine made of one compression and one expansion columns, an initial value of the pressure in the heater (H) is first assumed. Given this pressure, the compression and expansion cylinders instantaneous variables such as m, p, T, $\dot{m}_{adm}$, $\dot{m}_{exh}$ can be determined. The pressure in the heater is then adjusted until the cycle-averaged mass flowrate of the expansion cylinder equals the cycle-averaged mass flow rate of the compression cylinder.

The cycle averaged performances of the whole engine are then easily computed, given the effectiveness ε_R of the heat recovery exchanger (R).

The indicated work of the compression or expansion cylinder is obtained from:

$$W_{ind,j} = -\oint p\, \mathrm{d}V_j \qquad j = comp, exp, \qquad (12)$$

The net indicated work is defined as the difference between the indicated work delivered by the expansion cylinder and the indicated work needed for compression:

$$\left| W_{ind,net} \right| = \left| W_{ind,exp} \right| - W_{ind,comp}, \qquad (13)$$

The indicated mean pressure is often used for internal combustion engine. In the case of an Ericsson engine, with separate expansion and compression cylinders, it can be defined by reference to the expansion cylinder [4]:

$$imp = \frac{\left| W_{ind,net} \right|}{V_E}, \qquad (14)$$

with V_E the swept volume of the expansion cylinder, that is the difference between the maximum and the minimum (dead) volume. As there are 2 expansion cylinders in phase opposition, the net indicated work considered in (14) is the total work produced by the whole engine (both columns), and the expansion cylinder capacity is twice the swept volume of one expansion column.

Separate simulations are made for the left and the right columns of the whole engine. Indeed, due to the crankshaft mechanism (Equations (1) to (5)), the pressure in the right expansion or compression cylinder $p_{right}(\theta)$ is not exactly the same as the one in the left cylinder with a 180° phase shift $p_{left}(\theta$

+ π). The results for the whole engine (left and right compression and expansion columns) are then deduced from the results of both elementary engines.

2.2. Mechanical analysis

In the configuration considered, the total mass of liquid in motion in the engine is large. For instance, the mass of water in the expansion U tube (Fig. 2) corresponding to the data of Table 1 is 30 kg. The inertia force due to the motion of this mass can be important. Therefore it is necessary to evaluate the instantaneous forces acting on the solid pistons in the bottom of the U tubes of the expansion and compression spaces and the resulting torque on the crankshaft.

The instantaneous force on the solid piston at the bottom of each tube (compression and expansion) results from the force due to the working fluid pressure, the force due to the gravity, the force due to the liquid inertia and the force due to the pressure loss because of the friction of the liquid on the tube wall (14). The dissipation due to mechanical friction between solids parts of the engine is neglected, as the solid pistons are not in contact with the walls. A thin annular gap is allowed between the solid pistons and the tubes.

$$F_{piston} = F_{pressure} + F_{gravity} + F_{inertia} + F_{pressure\_loss}, \quad (15)$$

The force is assumed to be positive if it tends to push the solid piston towards the right.

The force due to the pressure is obtained by (16):

$$F_{pressure} = \frac{\pi D^2}{4}\left(p_{left} - p_{right}\right), \quad (16)$$

The force due to the gravity is given by equation (17):

$$F_{gravity} = \frac{\pi D^2}{4} 2\,\rho_l\, g\,(x - l), \quad (17)$$

where ρ_l is the density of the liquid and g is the acceleration of the gravity.

The force due to the inertia of the liquid in the tube is given by equation (18):

$$F_{inertia} = \frac{\pi D^2}{4} 2\,\rho_l\,\left(h_0 + l_0\right)\omega^2\,\frac{\mathrm{d}^2 x}{\mathrm{d}\theta^2}, \quad (18)$$

where h_0 is the height of the liquid column at equilibrium, and l_0 is half of the horizontal length of the tube (Fig. 2).

The evaluation of the force due the pressure loss because of the liquid friction on the cylinder wall is based on the assumption of quasi steady-state flow. For oscillating flows, this assumption is valid as long as the non-dimensional frequency ($\omega \rho D^2 / (4\,\mu)$) is low, which is not the case here. So the force due to the pressure loss computed from the quasi steady-state approach should be considered as an order of magnitude only, to compare with the other forces. The force due to the pressure loss is taken into account by means of a friction factor λ_f given by the Blasius law (19):

$$\lambda_f = 0.3164\, Re^{-0.25}, \quad (19)$$

where Re is the Reynolds number of the liquid, computed from the instantaneous piston velocity. The pipes used for the engine are made from PVC and PYREX, which can be assumed as hydraulically smooth. For the smallest rotational speed considered in this study, the Reynolds number of the liquid flow in the column, based on the mean liquid piston velocity is 4.5 10^4. So the Blasius law is relevant. The singular pressure loss due to the tube elbow is taken into account by considering an equivalent length of straight tube as in (20):

$$L_{eq,elbow} = 4\,D, \quad (20)$$

The equivalent total friction length is given by (21):

$$L_{tot} = 2\left(l_0 + h_0 + L_{eq,elbow}\right), \qquad (21)$$

The force due to the pressure loss is then obtained by (22):

$$F_{pressure\_loss} = \frac{\pi D^2}{4} \lambda_f \rho_l \frac{L_{tot}}{D} \frac{1}{2} \omega^2 \left|\frac{\mathrm{d}x}{\mathrm{d}\theta}\right| \frac{\mathrm{d}x}{\mathrm{d}\theta}, \qquad (22)$$

The total force on a solid piston is thus given by equation (23):

$$F_{piston} = \frac{\pi D^2}{4}\left(\left(p_{left} - p_{right}\right) + 2\rho_l g\left(x - l\right) + 2\rho_l \left(h_0 + l_0\right)\omega^2 \frac{\mathrm{d}^2 x}{\mathrm{d}\theta^2} + \lambda_f \rho_l \frac{L_{tot}}{D} \frac{1}{2} \omega^2 \left|\frac{\mathrm{d}x}{\mathrm{d}\theta}\right| \frac{\mathrm{d}x}{\mathrm{d}\theta}\right), \qquad (23)$$

The natural frequency of one U-shape column is obtained by cancelling the pressure and pressure loss forces and the force on the piston in equation (23). This leads to Eq (24):

$$0 = g\left(x - l\right) + \left(h_0 + l_0\right)\omega^2 \frac{\mathrm{d}^2 x}{\mathrm{d}\theta^2}, \qquad (24)$$

Considering a purely harmonic motion, this leads to the well-known natural frequency of a column of liquid oscillating in a U-tube (25):

$$2\pi f_0 = \omega_0 = \sqrt{\frac{g}{h_0 + l_0}}, \qquad (25)$$

The total force on the piston connecting rod results from the force exerted on the solid piston in the compression tube and the force on the solid piston in the expansion tube, as in (26):

$$F_{tot} = F_{piston,comp} + F_{piston,exp}, \qquad (26)$$

The instantaneous torque on the mechanical shaft can be deduced by equation (27):

$$C = -F_{tot} \frac{\mathrm{d}x}{\mathrm{d}\theta}, \qquad (27)$$

The torque is negative if it is resisting, and positive if the engine drives the flywheel.

3. Simulation results

The model is implemented in the MATLAB® language for technical computing. It runs on a laptop computer and the results are obtained in a few seconds. The presentation focuses on the influence of the rotational frequency on the force repartition applied to the piston and on the resulting torque. Indeed, for identical thermodynamic cycles in the cylinders, the mechanical power produced on the shaft of the engine is proportional to the rotation speed. In order to reduce the size of the system for a given shaft power, it is important to determine the maximum rotational speed which can be accepted. So three frequencies will be studied, ranging from the natural frequency f_0 to 5 f_0.

Table 2 presents the valve timing considered for each rotation speed. In order to obtain appropriate indicated diagrams and mass flowrates through the valves, the valve timing has to be slightly adapted when the rotation speed increases. Especially the inlet and exhaust valve closing angles of the expansion cylinder must be increased when the rotation speed increases. Indeed the volume of fluid which has to flow through the valves increases when the rotation speed increases.

Table 2. Valve timing

Compressor valve timing	n = 37.8 rpm		n = 75.7 rpm		n = 189.2 rpm	
	Left	Right	Left	Right	Left	Right
Inlet valve opening, IVO_{comp}	80°	246°	80°	267°	80°	267°
Inlet valve closing, IVC_{comp}	180°	0°	180°	0°	180°	0°
Exhaust valve opening, EVO_{comp}	304°	110°	305°	111°	307°	113°
Exhaust valve closing, EVC_{comp}	362°	182°	362°	182°	362°	162°
Expander valve timing						
Inlet valve opening, IVO_{exp}	1°	181°	1°	181°	1°	181°
Inlet valve closing, IVC_{exp}	60°	255°	60°	254°	60°	254°
Exhaust valve opening, EVO_{exp}	167°	347°	167°	347°	167°	347°
Exhaust valve closing, EVC_{exp}	290°	94°	290°	94°	294°	96°

3.1. Thermodynamics results

Fig. 3 presents the indicated (pressure – volume) diagrams of the compression space (a) and the expansion space (b) of the modelled engine for a rotational speed of 37.8 rpm, corresponding to the natural frequency of the oscillation of the liquid columns, f_0 = 0.63 Hz. The opening and closing timing of the valves are shown. The compressor indicated diagram is run counter-clockwise, meaning that a mechanical work has to be provided to the fluid by the liquid piston, while the expander indicated diagram is run clockwise, meaning that a mechanical work is provided by the fluid to the liquid piston.

The pressure evolutions are similar to those presented in the literature [19, 50, 52] and can be easily explained. For the compression cylinder, starting from the bottom dead centre, the pressure increases due to the motion of the piston towards the top dead centre. When the exhaust valve opens, the pressure continues to increase, because of the high speed of the piston and the low opening area of the valve. But a bit later, the speed of the piston decreases and the exhaust valve is open more largely so that the discharge occurs at nearly constant pressure. After the closure of the exhaust valve, the dead volume expands. When the inlet valve opens, the pressure continues to slightly decrease for the same reason as before: the piston motion tends to suck atmospheric air, but the valve is not yet fully open so that a slight depression is observed in the cylinder.

For the expansion cylinder, starting from the top dead centre, the working fluid is admitted at nearly constant pressure at first. But when the piston speed increases for the one hand, and the inlet valve begins to close for the other end, a larger pressure difference is created between the inlet pipe and the cylinder, so that the pressure in the cylinder begins to decrease. When the inlet valve is closed, the pressure decreases due to the piston motion towards the bottom dead centre. At this point the exhaust valve opens and the working fluid flows out of the cylinder at nearly constant pressure. But when the piston speed increases and the valve opening area decreases, the pressure in the cylinder begins to rise. After the exhaust valve closing, the dead volume working fluid is compressed up to the top dead centre.

The areas enclosed in the indicated diagram are equal to the indicated works. The area of the expansion indicated diagram is larger than the one of the compression indicated diagram, the difference corresponding to the net indicated work. The product of the indicated work times the rotation speed gives the indicated power.

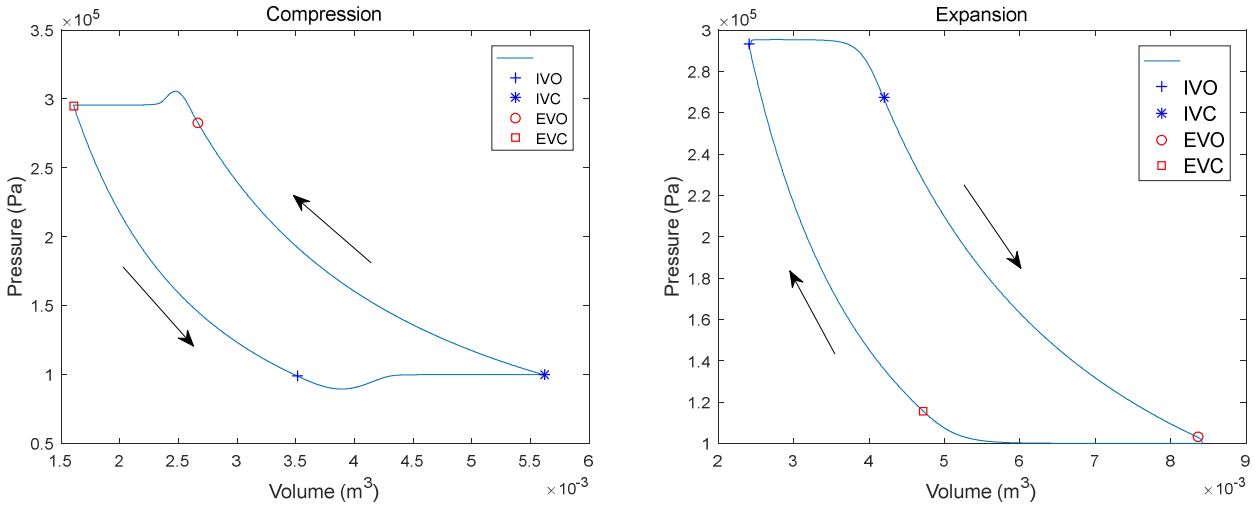

(a) (b)

Fig. 3. Indicated diagrams of the compression (a) and expansion (b) working spaces.

Fig. 4 presents the (temperature – volume) diagrams of the compression space (a) and the expansion space (b) of the modelled engine for the same rotational speed of 37.8 rpm. As the processes in the cylinder are assumed to be adiabatic, the global aspects of the figures are similar to the indicated diagrams.

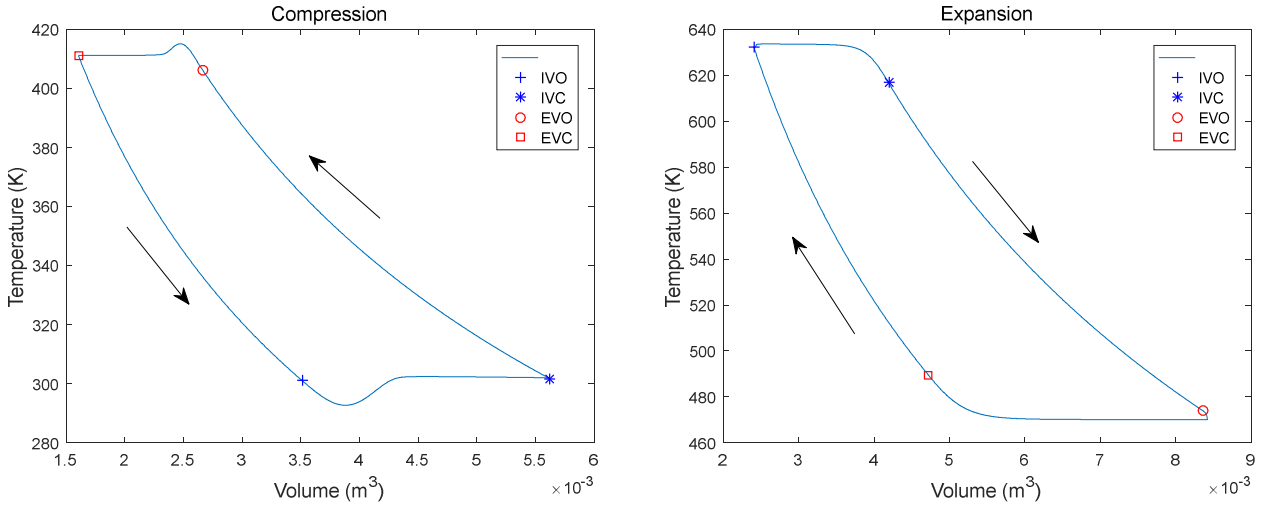

(a) (b)

Fig. 4. (T,V) diagrams of the compression (a) and expansion (b) working spaces.

Fig. 5 presents the mass flowrate of the working fluid through the inlet and exhaust valves of the compression working spaces (a) and the expansion working spaces (b). The high flow rates observed at the opening of the inlet and outlet valves of the compression cylinder are explained by the important pressure difference between the cylinder and the pipes at the start of the valve opening. A very small negative flow rate is observed at the start of the compression cylinder exhaust valve opening. This is due to the fact that at this angle, the pressure in the cylinder is slightly lower than the pressure in the outlet pipe. At the opening of the expansion cylinder exhaust valve a first peak of flow rate is observed. This is due to the fact that the pressure in the expansion cylinder is slightly higher than the atmospheric pressure when the valve begins to open. Of course, different valve opening and closure timings will lead to modified indicated diagrams and mass flow rates evolutions.

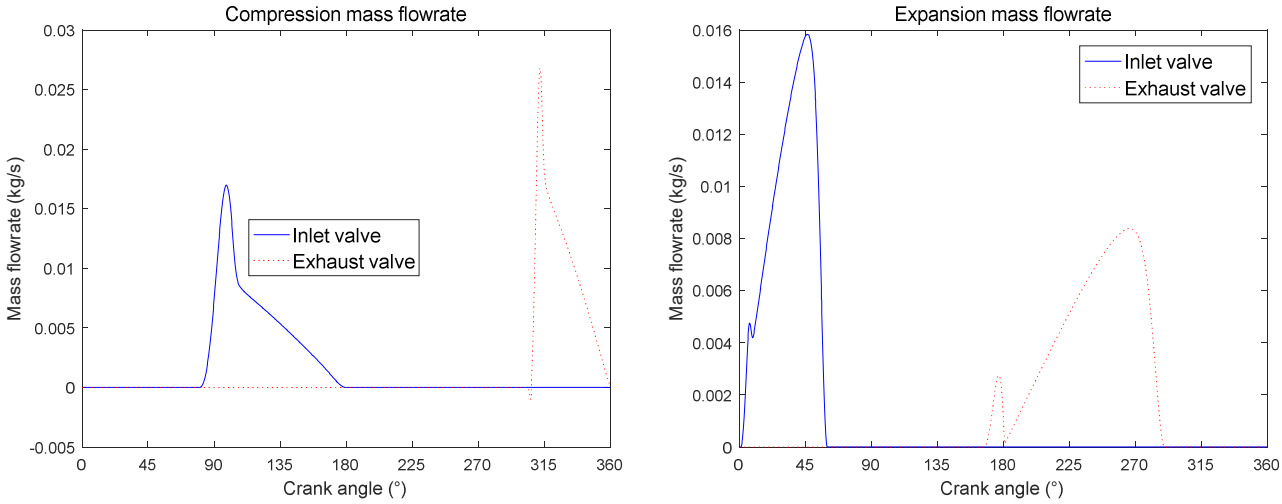

(a) (b)

Fig. 5. Mass flowrates through the valves of the compression (a) and expansion (b) working spaces.

Fig. 6 presents the entropy diagram of the cycle. This is the usual Joule cycle diagram, as the engine is assumed to run with two isentropic processes (compression k-cr and expansion h-er) and two isobaric processes (flow through the heat recovery exchanger cr-rh and the heater rh-h at pressure p_h and through the heat recovery er-rk and the exhaust rk-k at the atmospheric pressure p_k).

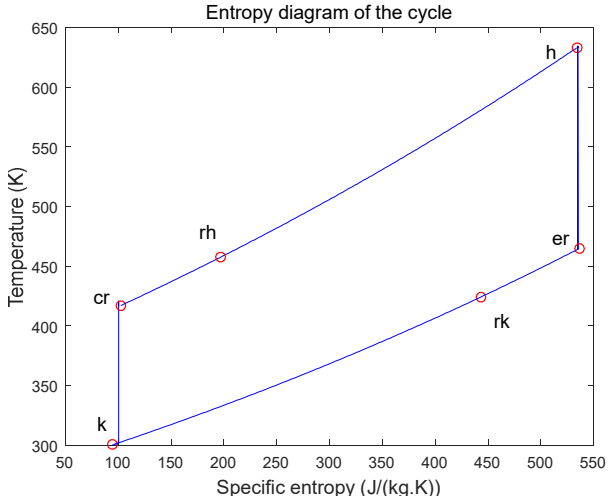

Fig. 6. Entropy diagram of the Ericsson engine cycle.

Table 3 presents the thermodynamics properties of the working fluid at the different locations in the engine for the rotational speed of 37.8 rpm.

Table 3. Thermodynamics properties of the working fluid in the cycle.

	T (K)	p (kPa)	h (kJ/kg)
k	300.0	100	26.94
cr	417.0	308.8	144.9
rh	457.5	308.8	186.2
h	633.2	308.8	368.8
er	464.6	100	193.5
rk	424.2	100	152.2

The general aspects of the (p, V) and (T, V) diagrams for the rotation speeds of 75.7 rpm (corresponding to 2 f_0) and 189.2 rpm (5 f_0) are similar to the ones obtained for 37.8 rpm.

Table 4 presents the global cycle performance of one elementary engine for f_0, 2 f_0 and 5 f_0. Due to the flow restriction through the valves, it can be seen that the mass flow rate is not proportional to the rotation speed. The expansion indicated work decreases when the rotation speed increases. Accordingly, the net indicated power of one elementary engine increases slower than the rotation speed and the efficiency decreases when the rotation speed increases.

Table 4. Thermodynamics performance of the cycle (whole engine).

n	p_H	$W_{ind,comp}$	$\lvert W_{ind,exp}\rvert$	$\lvert W_{ind,net}\rvert$	$\dot{W}_{ind,comp}$	$\lvert\dot{W}_{ind,exp}\rvert$	$\lvert\dot{W}_{ind,net}\rvert$	$\dot{Q}_H$	$\dot{m}$	η_{th}
rpm	kPa	J/cycle	J/cycle	J/cycle	W	W	W	W	g/s	-
37.8	295.3	546.8	840.2	293.4	344.8	529.8	185.0	527.5	3.083	0.3508
75.7	305.5	542.1	814.4	272.3	683.7	1027.0	343.4	1004.8	5.834	0.3418
189.2	316.9	528.1	750.0	221.9	1665.0	2364.5	699.5	2262.7	13.23	0.3092

3.2. Mechanical results

The instantaneous forces acting on the pistons and the instantaneous resulting torque on the crankshaft are computed for the three rotation speeds considered, in order to check if they are technologically acceptable.

Fig. 7 presents the instantaneous forces on the solid piston in the compression and in the expansion tubes at the rotational speed corresponding to the liquid column oscillation natural frequency. It can be seen that the forces due to the pressure of the working fluid (Eq. 16) are by far the most important. The gravity (Eq. 17) and the inertia (Eq. 18) forces are small, and they cancel each other since the rotational speed corresponds to the natural frequency. The force due to the pressure loss because of the friction of the liquid on the tube (Eq. 22) is negligible since the instantaneous velocity of the liquid columns is very small. Indeed, the maximum instantaneous velocity of the liquid piston is lower than 0.5 m/s. Therefore, the curves for the total force are nearly superimposed on the curves of the pressure evolution.

Considering the force on the compression solid piston (Fig. 7a), at $\theta = 0°$, the piston is on the left. The dead volume expands in the left compression cylinder while the working fluid is compressed in the right cylinder. At the beginning of the process, from $\theta = 0°$ up to $\theta = 58°$, the pressure in the left cylinder is higher than the pressure in the right cylinder, so that the resulting force is positive, pushing the compression piston towards the right. From $\theta = 58°$ up to $\theta = 180°$, the pressure in the right cylinder is higher than the one in the left cylinder, so that the resulting force is negative. At the end of this process, the force on the piston results from the admission at atmospheric pressure on the left, and the discharge at maximum pressure on the right cylinder. From $\theta = 180°$ up to $\theta = 360°$, the same processes occur, but pushing the piston in the opposite direction. The evolution of the force from $\theta = 180°$ up to $\theta = 360°$ is thus exactly the same than from $\theta = 0°$ up to $\theta = 180°$, but with the opposite sign.

Considering the force on the expansion solid piston (Fig. 7b), at $\theta = 0°$, the piston is on the left. The working fluid enters the left cylinder at high pressure while it flows out of the right cylinder at atmospheric pressure. So the force is maximum towards the right (positive force). The value of this force is larger than the corresponding force on the compression piston, because of the larger piston area in the expansion part of the engine. After the admission, when the piston goes on moving towards the right, the force decreases due to the expansion in the left cylinder and recompression of the dead volume in the right cylinder. From $\theta = 109°$ up to $\theta = 180°$, the pressure in the right cylinder during the process of recompression of the dead volume is higher than the pressure in the

left cylinder during the process of expansion of the working fluid. So the force is negative. From θ = 180° up to θ = 360°, the same processes occur, but pushing the piston in the opposite way. As for the compression piston, the evolution of the force from θ = 180° up to θ = 360° is thus exactly the same than from θ = 0° up to θ = 180°, but with the opposite sign.

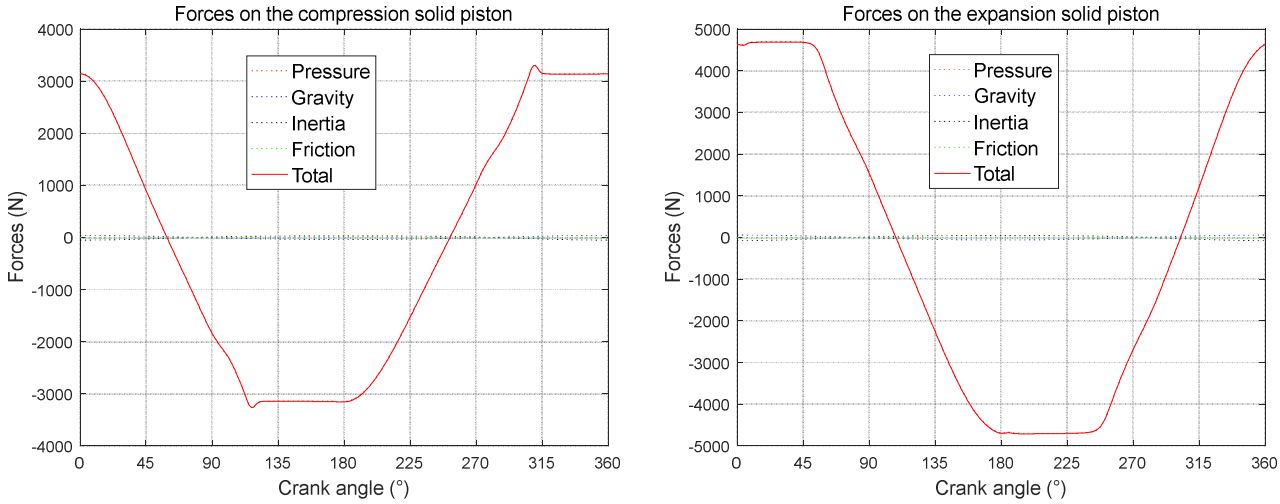

(a) (b)

Fig. 7. Forces on the compression (a) and expansion (b) solid pistons for the natural frequency rotational speed.

Fig. 8 presents the corresponding instantaneous torque on the shaft. The compressor, expander and total torques are equal to zero at θ = 0° and θ = 180°, which are the dead centres. Between θ = 0° and θ = 180°, and between θ = 180° and θ = 360°, the torques are positive at first (driving torque), then negative (resisting torque). The sign of the resulting torque on the flywheel changes four times per cycle. The mean resulting torque is positive.

It is possible to reduce the resistive torque on the flywheel by modifying the expansion cylinder valve timing. If the expansion exhaust valve closure EVC_{exp} is delayed up to the top dead centre, there is no recompression of the expansion dead volume, so, the resisting force and resisting torque from the expansion part of the engine vanish. The net shaft power of the engine is higher, but the efficiency is reduced [10, 51]

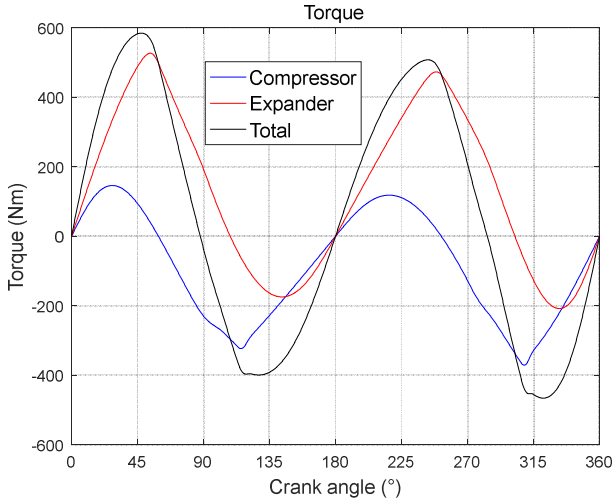

Fig. 8. Torques for the natural frequency rotational speed.

Fig. 9 presents the instantaneous forces on the solid piston in the compression and in the expansion tubes at the rotational speed corresponding to twice the liquid column oscillation natural frequency.

It can be seen that the inertia forces begins to grow, while the gravity and the friction force are still negligible. The inertia forces are maximum around each dead centre, when the flow reverses ($\theta = 0°$ and $\theta = 180°$). The evolution of the total forces on the pistons are very similar to the ones at the natural frequency (Fig. 7).

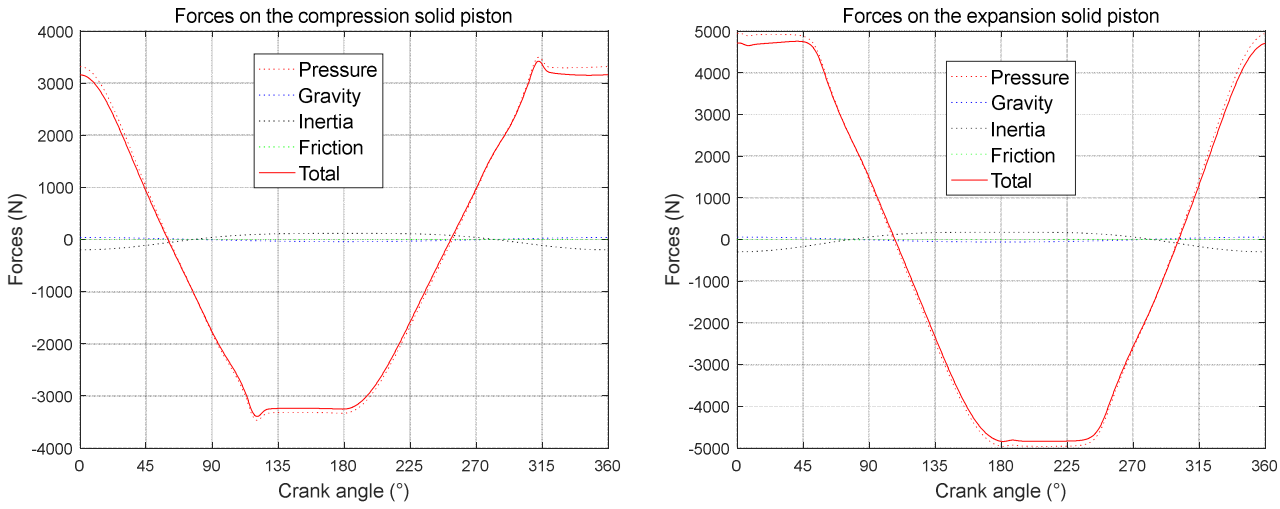

(a) (b)

Fig. 9. Forces on the compression (a) and expansion (b) solid pistons for twice the natural frequency rotational speed.

Fig. 10 presents the corresponding instantaneous torque on the shaft. The torque evolution at twice the natural frequency is very similar to the one at the natural frequency.

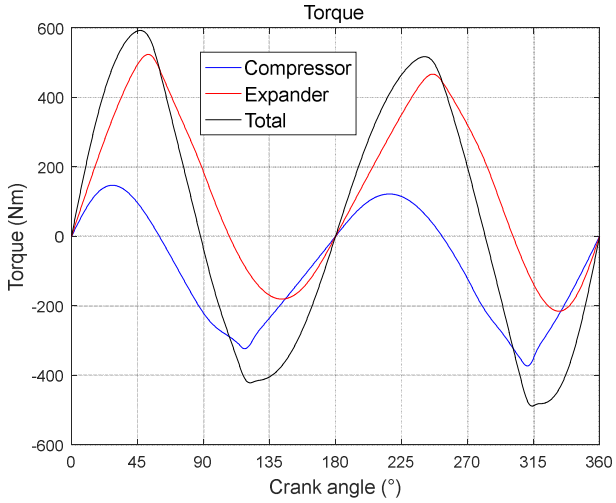

Fig. 10. Torques due to the compression and expansion solid pistons and total torque for twice the natural frequency rotational speed.

Fig. 11 presents the instantaneous forces on the solid piston in the compression and in the expansion tubes at the rotational speed corresponding to five times the liquid column oscillation natural frequency. It can be seen that the inertia forces are much larger, of the same order of magnitude as the pressure forces, while the gravity and the friction force are still negligible. The inertia force is globally in the opposite direction of the pressure force. So the effect of the inertia forces is to reduce the amplitude of the total forces variations.

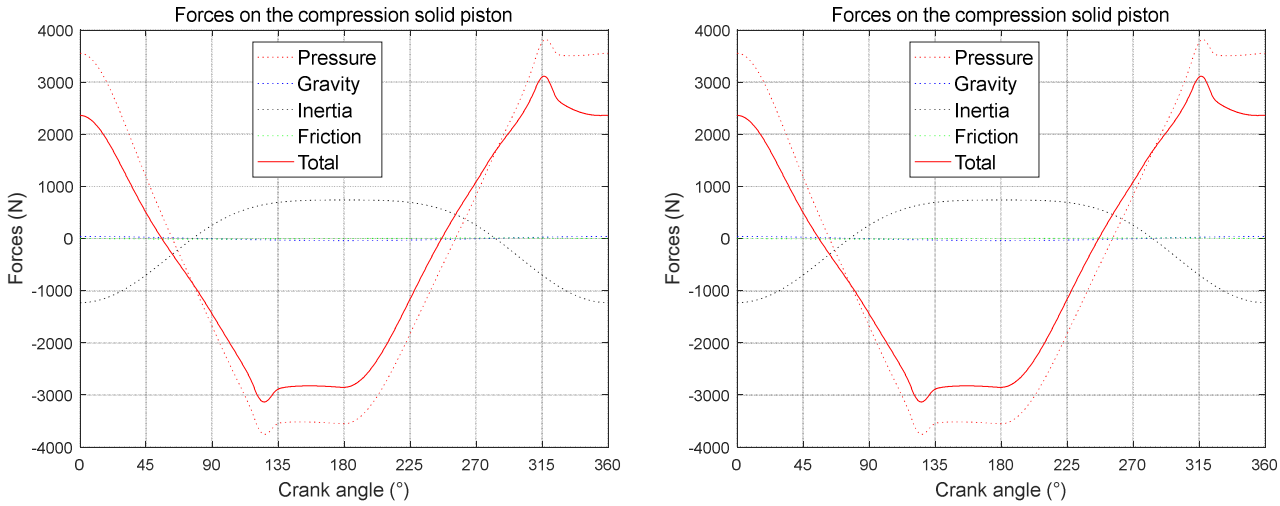

Fig. 11. Forces on the compression (a) and expansion (b) solid pistons for five times the natural frequency rotational speed.

Fig. 12 presents the corresponding instantaneous torque on the shaft. The global aspect of the evolutions of the torques during one cycle are similar to the ones at f_0 and $2f_0$ but the amplitudes of the torque variations on a cycle are reduced, as well as the maximum value of the total resisting torque. In the expansion part of the engine, the inertia of the liquid piston reduces the driving torque during the expansion of the working fluid, but helps to recompress the dead volume. In the compression part of the engine, the inertia of the liquid piston reduces the driving torque during the expansion of the dead volume, but helps the compression of the working fluid.

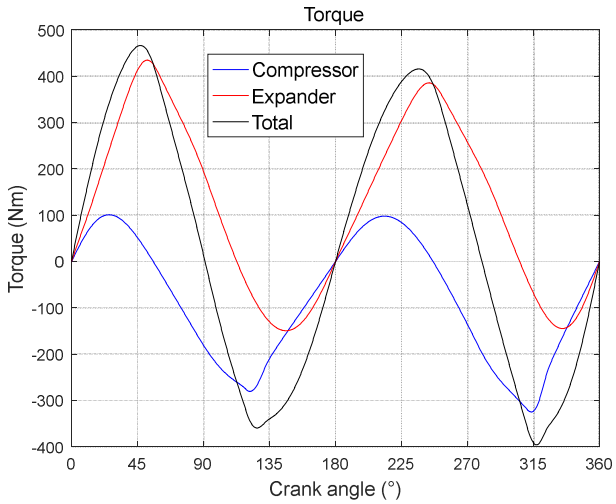

Fig. 12. Torques due to the compression and expansion solid pistons and total torque for five times the natural frequency rotational speed.

Table 5 presents the values of the mean torque on the flywheel. It can be seen that the resulting torque decreases as the rotational speed increases. The indicated mean pressure *imp* is quite low, due to the low pressure ratio of 3 chosen for the engine. It decreases when the rotation speed increases. The indicated power and the shaft power are also presented. The difference between the indicated power and the shaft power is due to the power dissipated by the liquid friction on the tube walls. It can be seen that the power dissipated by friction is negligible at low frequency while it represents about 4 % of the indicated power at five times the natural frequency of the liquid columns.

Table 5. Cycle averaged torque, indicated mean pressure and powers as a function of the rotational speed.

n (rpm)	37.83	75.67	189.2
C_{tot} (Nm)	46.64	43.08	33.95
imp (10^5 Pa)	0.244	0.226	0.185
$\left\|\dot{W}_{ind,net}\right\|$ (W)	185.0	343.4	699.5
$\left\|\dot{W}_{shaft}\right\|$ (W)	184.8	341.3	672.5

5. Conclusion

An innovative configuration of an Ericsson engine is presented. This configuration is assumed to be easier to build than conventional mechanical engines and to be suited for small scale conversion of biomass or solar energy into mechanical or electrical energy. A model is developed in order to evaluate the instantaneous temperatures and pressures in the compression and expansion chambers of the engine and to predict the instantaneous forces on the piston rods and torques on the shaft. The model has been used to predict the performance of a prototype under construction.

It is shown that the engine indicated efficiency decreases when the rotation speed increases. As recompression of the expansion space dead volume is considered for efficiency reasons, the sign of the instantaneous torque on the flywheel changes four times per cycle, calling for a heavy flywheel. When the rotation speed corresponds to the natural frequency of the columns of liquid, the instantaneous torque on the flywheel is due to the pressure forces only. When the rotation speed increases, the influence of the liquid pistons inertia is growing. Its impact is globally opposite to the one of the pressure. So when the rotation speed increases above the natural frequency of the liquid columns, the effect of the inertia of the liquid columns is to reduce the amplitude of the torque variations.

References

[1] International Energy Agency, 2014 Annual Report, https://www.iea.org/publications/.../2014_IEA_AnnualReport.pdf

[2] Finkelstein Th, Organ AJ. Air engines. London: Professional Engineering Publishing Ltd; 2001.

[3] Stouffs P. Hot Air Engines. Journal of Applied Fluid Mechanics 2011;4:1–8.

[4] Creyx M, Delacourt E, Morin C, Desmet B, Peultier P. Energetic optimization of the performances of a hot air engine for micro-CHP systems working with a Joule or an Ericsson cycle. Energy 2013;49:229–239.

[5] Bonnet S, Alaphilippe M, Stouffs P. Energy, exergy and cost analysis of a micro-cogeneration system based on an Ericsson engine. Int J Therm Sci 2005; 44/12:1161–8.

[6] Touré A. Etude théorique et expérimentale d'un moteur Ericsson destiné à la microcogénération. PhD thesis, Pau: UPPA; 2010.

[7] Alaphilippe M., Bonnet S., Stouffs P., Low power thermodynamic solar energy conversion: coupling of a parabolic trough concentrator and an Ericsson engine, Int. J. of Thermodynamics, N° 10, p. 37-45, 2007.

[8] Le Roux WG, Bello-Ochende T, Meyer JP. A review on the thermodynamic optimisation and modeling of the solar thermal Brayton cycle. Renewable and sustainable energy reviews 2013;28:677–690.

[9] Ndamé Ngangué M., Stouffs P., Modelling of a Uniflow hot air engine, Proceedings of the 17th International Stirling Engine Conference (ISEC) Newcastle, Northumbria University, (August 24-26, 2016).

[10] Touré A., Stouffs P., Modeling of the Ericsson engine, Energy, Volume 76, 1 November 2014, p. 445-452.

[11] C. D. West, The Fluidyne heat engine. AERE R6775, UKAEA Atomic Energy Research Establishment, Harwell, UK, 1971.

[12] C. D. West, R. B Pandey. A laboratory prototype Fluidyne water pump. In: Proceedings of 16th intersociety energy conversion engineering conference, Atlanta, GA, USA, 1981. [11] C. D. West, Liquid piston Stirling engines. New York, USA: Van Nostrand Reinhold Company, 1983.

[13] C. D. West, Dynamic analysis of the Fluidyne. In: Proceedings of 18th intersociety energy conversion engineering conference, Orlando, Florida, USA, p. 830812-830849, 1983.

[14] D. C. Mosby, The fluidyne heat engine, Master thesis Monterey, California. Naval Postgraduate School, California USA, 1978.

[15] G. T. Reader and P. D. Lewis, Modes of operation of a jet-stream Fluidyne. In: Proceedings of 14th intersociety energy conversion engineering conference, Boston, MA, USA; p. 1098-1102, 1979.

[16] G. C. Bell, Solar powered liquid piston Stirling cycle irrigation pump. U.S. Department of Energy, Solar Energy, 29 pages, 1979.

[17] L. F. Goldberg, C. J. Rallis, A prototype liquid-piston free-displacer Stirling engine. In: Proceedings of 14th intersociety energy conversion engineering conference, Boston, MA, USA, p. 1103-8, 1979.

[18] Y. Shahabasi, Fluidyne Heat Engine Construction and Performance. Journal of agriculture of University of Puerto Rico, 1985.

[19] F. K. M. Aloysius Obodoako and C. Everbach, Design and Development of a liquid piston Stirling engine. E90 Senior Design Project Report, May 2006.

[20] J. Van de Ven, P. Gaffuri, B. Mies, and G. Cole, Developments towards a liquid piston Stirling engine. In International Energy Conversion Engineering Conference, Cleveland, Ohio, 2008.

[21] J. D. Van de Ven, Mobile hydraulic power supply: Liquid piston Stirling engine pump, Renew. Energy, vol. 34, n°11, pp. 2317-2322, Nov. 2009.

[22] N. Yang, R. Rickard, K. Pluckter, and T. Sulchek, Integrated two-cylinder liquid piston Stirling engine. Appl. Phys. Lett., vol. 105, n°14, p. 143903 (1-4), Oct. 2014.

[23] J. W. Mason and J. W. Stevens, Characterization of a solar-powered fluidyne test bed, Sustain. Energy Technol. Assess., vol. 8, pp. 1-8, Dec. 2014.

[24] S. Narayan, A. Gupta, and R. Rana, Performance analysis of liquid piston Fluidyne systems. Mech. Test. Diagn., vol. 2, p. 12-18, 2015.

[25] S. Narayan, V. Gupta, Motion analysis of liquid piston engines. Journal of Engineering Studies and Research, vol. 21, nº 2, pp. 71-77, 2015.

[26] G. B. De Klerk, C. J. Rallis, A solar powered, back-to-back liquid piston Stirling engine for water pumping. Journal of Energy in Southern Africa, vol. 13, n°2, p. 36-42, 2002.

[27] R. P. Klüppel, J. M. Gurgel, Thermodynamic cycle of a liquid piston pump. Renew. Energy, vol. 13, n°2, pp. 261-268, 1998.

[28] E. Orda, K. Mahkamov, Development of “Low-tech” solar thermal water pumps for use in developing countries. J. Sol. Energy Eng. - Trans ASME, vol 126, p.768-773, 2004.

[29] H. Jokar and, A. R. Tavakolpour-Saleh, A novel solar-powered active low temperature differential Stirling pump, Renew. Energy, vol. 81, pp. 319-337, Sep. 2015.

[30] S. Yatsuzuka, Y. Niiyama, K. Fukuda, K. Muramatsu, and N. Shikazono, Experimental and numerical evaluation of liquid-piston steam engine. Energy, vol. 87, pp. 1-9, Jul. 2015.

[31] C. Piya, Liquid Piston Gas Compression. A Major Qualifying Project Report, Worcester Polytechnic Institute, 2009.

[32] J. D. Van de Ven and P. Y. Li, Liquid piston gas compression. Appl. Energy, vol. 86, n°10, pp. 2183-2191, Oct. 2009.

[33] C. Piya, I. Sircar, J. D. Van de Ven, and D. J. Olinger, Numerical Modeling of Liquid Piston Gas Compression. ASME 2009 International Mechanical Engineering Congress and Exposition, pp. 507-517, 2009.

[34] N. Kumar, M. Hofacker, and E. Barth, Design and Control of a Free-Liquid-Piston Engine Compressor for Compact Robot Power. Vanderbilt Undergraduate Research Journal VURJ, vol. 9, 2013.

[35] C. Vikram Patil, A. Pinaki, P. I. Ro, Experimental investigation of heat transfer in liquid piston compressor. Applied Thermal Engineering, vol. 146 p. 169-179, 2019.

[36] T.C.B. Smith. Power dense thermofluidic oscillators for high load applications. In: Proceedings of 2nd International Energy Conversion Engineering Conference. Providence, Rhode Island, 2004.

[37] T.C.B. Smith. Asymmetric heat transfer in vapour cycle liquid-piston engines. In: Proceedings of 12th International Stirling Engine Conference, Durham,. p. 302-314, UK. 2005.

[38] C. N. Markides and T. C. B. Smith, A Dynamic Model for the Efficiency Optimization of an oscillatory low grade heat engine. Energy, vol.36, p. 6967-6980, 2011.

[39] R. Solanki, A. Galindo, and C. N. Markides, Dynamic modelling of a two-phase thermofluidic oscillator for efficient low grade heat utilization: Effect of fluid inertia. Appl. Energy, vol. 89, n°1, pp. 156-163, 2012.

[40] C. N. Markides, A. Osuolale, R. Solanki, and G.-B. V. Stan, Nonlinear heat transfer processes in a two-phase thermofluidic oscillator. Appl. Energy, vol. 104, pp. 958-977, Apr. 2013.

[41] R. Solanki, A. Galindo, C. N. Markides, The role of heat exchange on the behaviour of an oscillatory two-phase low-grade heat engine. Appl. Therm. Eng., vol. 53, n°2, pp. 177-187, May 2013.

[42] R. Solanki, R. Mathie, A. Galindo, C. N. Markides, Modelling of a two-phase thermofluidic oscillator for low-grade heat utilisation : Accounting for irreversible thermal losses. Appl. Energy, vol. 106, p. 337-54, 2013.

[43] C. N Markides, A. Gupta, Experimental investigation of a thermally powered central heating circulator: pumping characteristics. Appl Energy, vol. 110, p. 132-146, 2013.

[44] C. N Markides, R. Solanki, A. Galindo, Working fluid selection for a two-phase thermofluidic oscillator: effect of thermodynamic properties. Appl. Energy, vol. 124, p. 167-185, 2014.

[45] S. Mauran, M. Martins, D. Stitou et H. Semmari. A novel process for engines or heat pumps based on thermal-hydraulic conversion. Applied Thermal Engineering, vol. 37, p. 249-257, May 2012.

[46] M. Martins, S. Mauran, D. Stitou, P. Neveu. A new thermal-hydraulic process for solar cooling. Energy, vol. 41, p. 104-112, 2012.

[47] K. Mahkamov, E. Orda, B. Belgasim, I. Makhkamova, A novel small dynamic solar thermal desalination plant with a fluid piston converter. Applied Energy, vol 156, p. 715-726, 2015.

[48] M. Ndamé Ngangué, O. Sosso Mayi, P. Stouffs, Study of Three Valves Command Laws of The Expansion Cylinder of a Hot Air Engine, International J. of Thermodynamics, vol. 22 (No. 2), pp. 84-96, 2019.

[49] Wojewoda, Z. Kazimierski, Numerical model and investigations of the externally heated valve Joule engine. Energy, vol 35, p. 2099-2108, 2010.

[50] F. Lontsi, O. Hamandjoda, K. Fozao, P. Stouffs, J. Nganhou, Dynamic simulation of a small modified Joule cycle reciprocating Ericsson engine for microcogeneration systems. Energy, vol. 63, p. 309-316, 2013.

[51] M. Creyx, E. Delacourt, C. Morin, and B. Desmet, Dynamic modelling of the expansion cylinder of an open Joule cycle Ericsson engine: A bond graph approach. Energy, vol. 102, pages 31-43, March 2016.

[52] D. Stanciu and V. Bãdescu, Solar-driven Joule cycle reciprocating Ericsson engines for small scale applications. From improper operation to high performance. Energy Conversion and Management, vol 135, p. 101-116, 2017.

[53] M. Motamedi, R. Ahmadi, and H. Jokar, A solar pressurizable liquid piston Stirling engine: Part 1, mathematical modeling, simulation and validation. Energy, vol. 155, pages 796-814, 2018.

Nomenclature

a crank radius, m
A instantaneous flow area through the valve, m²
C compression cylinder
C instantaneous torque, Nm
C_d flow coefficient, -
D Diameter of the tube, m
E expansion cylinder
F force, N
f_o natural frequency, s^{-1}
g acceleration of the gravity, $m.s^{-2}$
H heater
h enthalpy per unit mass, $J.kg^{-1}$
h_o equilibrium liquid height of the column, m
imp indicated mean pressure, Pa
k $= (\gamma - 1) / \gamma$, -
l connecting rod length, m
L length, m
l_o horizontal tube length, m
m mass of air, kg
$\dot{m}$ mass flow rate, $kg.s^{-1}$
n rotation speed s^{-1}
p pressure, Pa
Q heat, J
$\dot{Q}$ thermal power, W
r perfect gas constant, $J.kg^{-1}.K^{-1}$
R pressure ratio, -
R heat recovery exchanger
RA buffer storage
Re Reynolds number, -
T temperature, K
t time, s
TDC Top Dead Center
u internal energy, $J.kg^{-1}$
V flywheel
V volume, m^3
w specific work, $J.kg^{-1}$
W work, J
$\dot{W}$ mechanical work, W
x position of the piston, m

Greek symbols

γ c_p / c_v , -
ε_R heat recovery exchanger effectiveness, -
ζ_d relative dead volume, -
λ ratio of the connecting rod length to the crank radius, -
λ_f friction factor, -
ω angular speed, s^{-1}
ω_o natural angular speed, s^{-1}
ρ fluid density, $kg.m^3$
θ instantaneous crank angle, -

Subscripts

adm admission
comp compression
cr fluid state between C and R
crit critical
elbow tube elbow
eq equivalent
er fluid state between E and R
exh exhaust

exp	expansion
gravity	gravity
h	fluid state at the outlet of H
i	refers to *C* or *E*
ind	indicate
inertia	inertia
k	ambient state at the compressor inlet
left	left
l	liquid
net	net
piston	piston
*pressur*e	pressure
pressure_loss	pressure loss
R	recovery
rh	fluid state between R and H
right	right
rk	fluid state at the outlet of R (exhaust)
th	thermal
tot	total